4th International Conference on
Earthquake Geotechnical Engineering
June 25-28, 2007
Paper No. 1740

SEISMIC BEHAVIOR OF 2D SEMI-SINE SHAPED HILLS SUBJECTED TO VERTICALLY PROPAGATING INCIDENT SV AND P WAVES

Mohsen KAMALIAN[1], Mohammad Kazem JAFARI[2], Abdollah SOHRABI-BIDAR[3], Arash RAZMKHAH[4]

ABSTRACT

This paper presents the preliminary results of an extensive numerical parametric study on seismic behavior of two-dimensional homogenous semi-sine shaped hills subjected to vertically propagating incident SV and P waves. The medium is assumed to have a linear elastic constitutive behavior. All calculations are executed in time-domain using the direct boundary element method. Clear perspectives of the amplification patterns of the hill are presented by investigation of the frequency-domain responses. It is shown that wave length, site geometry and in a less order of importance, wave type and Poisson's ratio, are the independent key parameters governing the hill's amplification pattern. Simple formula and tables are proposed for estimating the characteristic site period and also the average amplification factors of the semi-sine shaped hills, which could be applied in site effect microzonation studies of topographic areas.

Keywords: Semi-sine Hill, Characteristics Period, Microzonation, Topography Effect, BEM

INTRODUCTION

In the recent past there have been numerous cases of recorded motion and observed earthquake damage pointing toward topographic amplification as an important effect. Very high acceleration recorded at Pacoima Dam (1.25g) during the 1971 San Fernando earthquake (Trifunac and Hudson, 1971; Boore, 1973) and Tarzana hill (1.78g) during the 1994 Northridge earthquake (Spudich et al., 1996) have been at least partly attributed to topographic effects. Observations from the 1983 Coalinga earthquake (Celebi, 1991), the 1985 Chile earthquake (Celebi, 1987), the 1987 Superstition Hills earthquake (Celebi, 1991) as well as observations from recent earthquakes in Greece (Athanasopoulos et al., 1999; Bouckovalas and Kouretzis, 2001) are only some examples of catastrophic events, during which severe structural damage has been reported on high elevated regions.

Although nowadays it is well established that the seismic ground response of surface topographies could be different compared to those of the free field motion during earthquakes, but there are only few structural codes which have considered this issue (AFPS90; Eurocode8). This is due to complex nature of the seismic wave scattering by topographical structures which can only be solved accurately, economically and under realistic conditions, by advanced numerical methods. A recent compilation of

[1] Assistant Professor, Geotechnical Engineering Research Center, International Institute of Earthquake Engineering and Seismology, I.R. Iran, Email: kamalian@iiees.ac.ir
[2] Associated Professor, Geotechnical Engineering Research Center, International Institute of Earthquake Engineering and Seismology, I.R. Iran, Email: jafari@iiees.ac.ir
[3] Ph.D. Student, Seismology Research Center, International Institute of Earthquake Engineering and Seismology, I.R. Iran, Email: sohrabi@iiees.ac.ir
[4] Assistant Professor, South Tehran Branch, Islamic Azad University, I.R. Iran, Email: ar.razm@iiees.ac.ir

works on the numerical modeling of seismic wave propagation has been presented by Bard (1994), Beskos (1997) and Sanchez-Sesma et al. (2002).

Semi-sine shaped hills are one of the most popular surface irregularities. Bouchon (1973) was the first who investigated the seismic response of semi-sine shaped hills subjected to incident SH, SV and P waves, using the well known frequency domain Aki and Larner method (Aki and Larner, 1970). In the case of SH waves, he carried out an interesting parametric study, including hills with different shape ratios (ratio of height to half width of the hill) of 0.23 to 0.8, subjected to incident waves with wave lengths of 5.0 times the height of the hill. The most important result achieved was that near top of the hill, the amplification factor increases proportional with the shape ratio.

Geli et al. (1988) reviewed the published results of experimental and numerical studies made on seismic behavior of topographic structures. They studied by use of the Aki and Larner method the amplification patterns of some complex configurations of 2D topographic futures subjected to incident SH waves, considering different predominant dimensionless frequencies. The dimensionless frequency defined as the ratio of the width of the hill to the shear wave length, was evaluated as $\Omega=\omega b/\pi c_2$, where ω presents the angular frequency of the wave, and b and c_2 denote the half width and shear wave velocity of the hill. They showed that in the case of 2D semi-sine shaped hills with a shape ratio of 0.4, incident waves with dimensionless frequencies of less than 2.5 would be solely amplified at the top of the hill, and alternately amplified / de-amplified on the base of the hill.

Bouchon et al. (1996) used a semi-analytical / semi-numerical method, based on discrete wave number Green functions and boundary integral equations in the frequency domain, in order to study the diffraction phenomena of elastic waves by three-dimensional hills. They evaluated the seismic response of a 3D semi-sine shaped hill, which had an elliptic shaped base with two shape ratios of 0.2 and 0.4 for the major and minor axis, respectively, against incident shear waves with different wave lengths. They showed that in the case of incident waves with wave lengths of greater than the height of the hill, the amplification factor at the top of the hill would be always greater than one, increase inversely with the wave length and reach its maximum for a wave length of equal to the height of the hill. Komatitsch and Vilotte (1998) solved the same problem by spectral element method and got consistent results.

Review of the literature shows that perfect parametric studies on seismic behavior of 2D hills subjected to incident SV and P waves have been seldom published. The published works were either limited to the simple case of incident SH waves or were restricted to some specific values of shape ratio and dimensionless frequency. Furthermore, some interesting parametric analyses made recently by Ashford et al. (1997) and Bouckovalas and Papadimitriou (2005) on the topography effect were restricted to the slope sections and did not consider the hills. This paper presents the preliminary results of a numerical parametric study on amplification pattern of 2D homogenous semi-sine shaped hills subjected to vertically propagating incident SV and P waves, using time-domain boundary element (BE) method. Assessing the effects of site geometry, wave characteristics and material parameters on the 2D homogenous semi-sine shaped hill's response and obtaining simple rules for seismic microzonation of topographic areas were the two essences of this paper.

METODOLOGY

The geometry of the 2D homogenous semi-sine shaped hills (figure 1) investigated by the parametric study was defined as follows:

$$\xi(x)=\begin{cases}0.5h(1+\cos(\pi x/b)) & |x|\le b\\ 0 & |x|>b\end{cases} \quad (1)$$

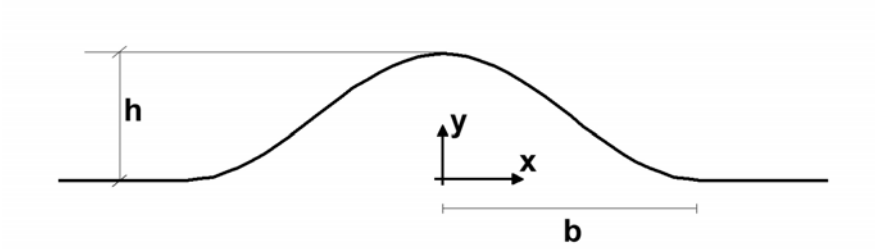

Figure 1. Geometry of the studied 2D homogenous semi-sine shaped hill

where b and h denote the half-width and height of the hill, respectively.

The parametric study was mainly aimed to find out the answers of the following questions: What is the maximum amplification potential of the hill? Where does it occur along the hill? How does the amplification pattern vary along the hill? How does it depend on the height and width of the hill? How does it depend on the length of the incident wave and the Poisson's ratio? All amplification factors were defined with respect to the free field (twice the incident) motion and were calculated as the ratio of the Fourier amplitude of the horizontal (or vertical) motion to the Fourier amplitude of the free field motion.

In order to find out the answers of the above mentioned questions, the hill was subjected to the vertically propagating Ricker type SV and P wave:

$$f(t) = \left[1 - 2 \cdot (\pi \cdot f_p \cdot (t - t_0))^2\right] e^{-(\pi \cdot f_p \cdot (t - t_0))^2} \tag{2}$$

where f_p and t_0,which denote the predominant frequency and an appropriate time shift parameter, respectively. All results were presented in dimensionless forms, using the well known dimensionless period $T = \pi c_2 / \omega b$ (or its inverse: the dimensionless frequency), which means physically the ratio of the incident's wave length to the width of the hill. Seven different shape ratios (h/b) of 0.1, 0.2, 0.3, 0.4, 0.5, 0.6 and 0.7 as well as four different Poisson's ratios of 0.1, 0.2, 0.33 and 0.4 were considered. Based on engineering interests, a dimensionless period interval of 0.25 to 8.33 was considered, which corresponds to incident waves with wave lengths of 0.25 to 8.33 times the hill's width. This broad period interval was divided into the following five subintervals: 0.25 to 0.50 (P1), 0.50 to 1.00 (P2), 1.00 to 2.00 (P3), 2.00 to 4.17 (P4) and 4.17 to 8.33 (P5), corresponding to incident waves with very short, short, medium, large and very large wave lengths, respectively. For the reason of simplicity and following the well known concept of average horizontal spectral amplification (AHSA) defined by Borcherdt et al. (1994) as spectral ratios representing averages over short, intermediate, mid and long period bands, five distinct amplification factors were computed for every point along the hill, by averaging the corresponding amplification curve over each of the above mentioned five period subintervals P1 to P5.

The parametric study was executed by solving the following well known transient boundary integral equation governing the dynamic equilibrium of isotropic elastic media:

$$c_{ij}(\xi) \cdot u_i(\xi, t) = \int_{\Gamma} \left(G_{ij} * t_i(x,t) - F_{ij} * u_i(x,t)\right) \cdot d\Gamma \tag{3}$$

in which u_i denotes the displacement vector and t_i represents the traction at the boundary. G_{ij} and F_{ij} are the transient displacement and traction kernels, respectively, and represent the displacements and tractions at a point x at time t due to a unit point force applied at ξ and at the preceding time τ. The terms $G_{ij}*t_i$ and $F_{ij}*u_i$ are the Riemann convolution integrals and c_{ij} denotes the well known discontinuity term resulting from the singularity of the F_{ij} kernel. The BE formulation of equation 3

was implemented in a general purpose two-dimensional nonlinear two-phase BEM/FEM code named as HYBRID (Kamalian, 2001). Several examples were solved in order to show the accuracy and efficiency of this implemented BE algorithm in carrying out site response analysis of topographic structures (Kamalian et. al, 2003; 2006).

GENERAL AMPLIFICATION PATTERN

Figures 2 demonstrates clear perspectives of the amplification patterns of a 2D semi-sine hill, with a shape ratio of 0.5 and a Poisson's ratio of 0.33, subjected to incident SV and P waves, at receiving points arranged within an interval of $-4b$ to $4b$ from the origin. As can be seen:

At any point along the ground surface, the free field motion is amplified (or deamplified) and both components of motion exist. The amplification patterns, which consist of frequencies of amplifications and deamplification, are gradual and smooth, due to gentle variations of the slope along the hill. Each amplification pattern shows a characteristic frequency (or characteristic period), at which all points along the hill have amplification factors of greater than one and show in-phase motions. The amplification curve of the hill due to its characteristic frequency finds its maximum at the crest and decays toward the bases. If the incident wave has a frequency of smaller than the characteristic frequency of the hill, decreasing the wave's frequency reduces the hill's effect on the ground surface response. In other words, if the hill is impinged by incident waves with wave lengths of much greater than the hill's width, the ground surface response would be approximately the same as the well known free field motion.

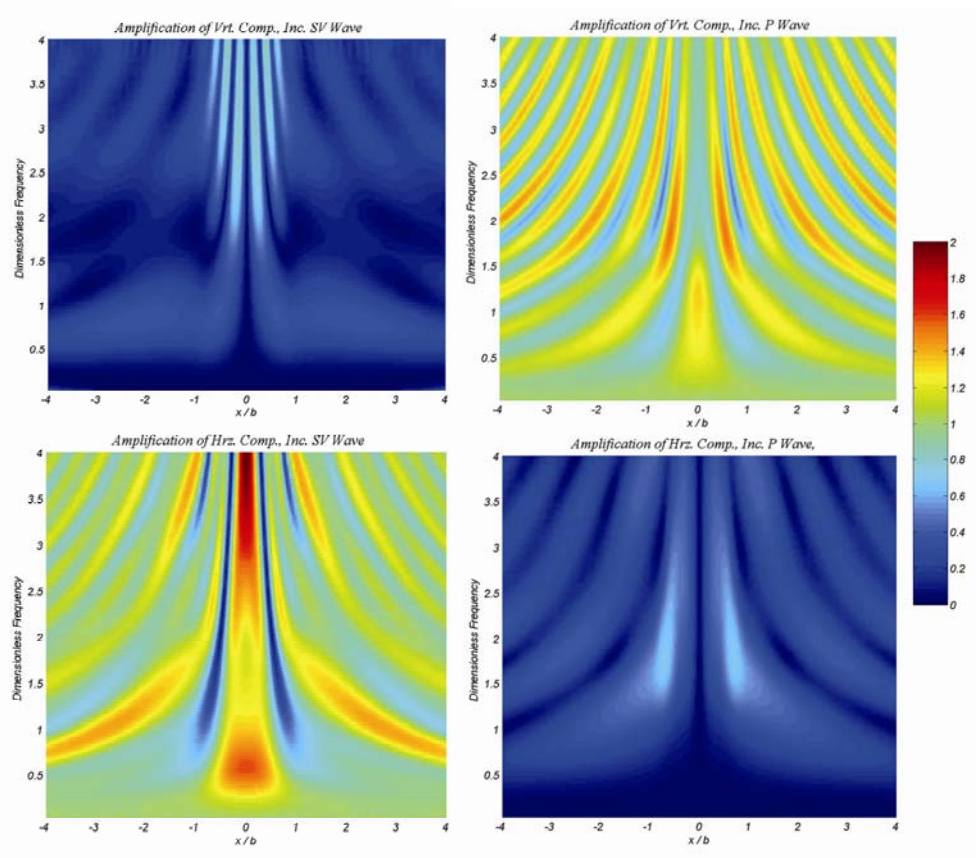

Figure 2. Amplification patterns of a semi-sine shaped hill with shape ratio of 0.5 in case of incident SV (left) and P (right) waves

RESULTS OF PARAMETRIC ANALYSIS

This section presents the results of the executed parametric study, which demonstrates the sensitivity of 2D semi-sine shaped hill's amplification patterns on key parameters such as shape ratio, wave length of the incident wave, wave type and Poisson's ratio.

Shape Ratio Effect

Figure 3 categorizes the amplification patterns of 2D semi-sine shaped hills with a Poisson's ratio of 0.33, subjected to vertically incident SV waves, according to their wave lengths. Both of horizontal and vertical components of amplification are shown. Although the amplification potential of the hill increases in general with the shape ratio, but the increasing rate depends on the wave length and varies across the hill. Figure 4 compares the amplification curve at the crest of the hill versus different shape ratios. As can be seen, increasing the shape ratio increases the characteristic period of the hill and its corresponding amplification factor.

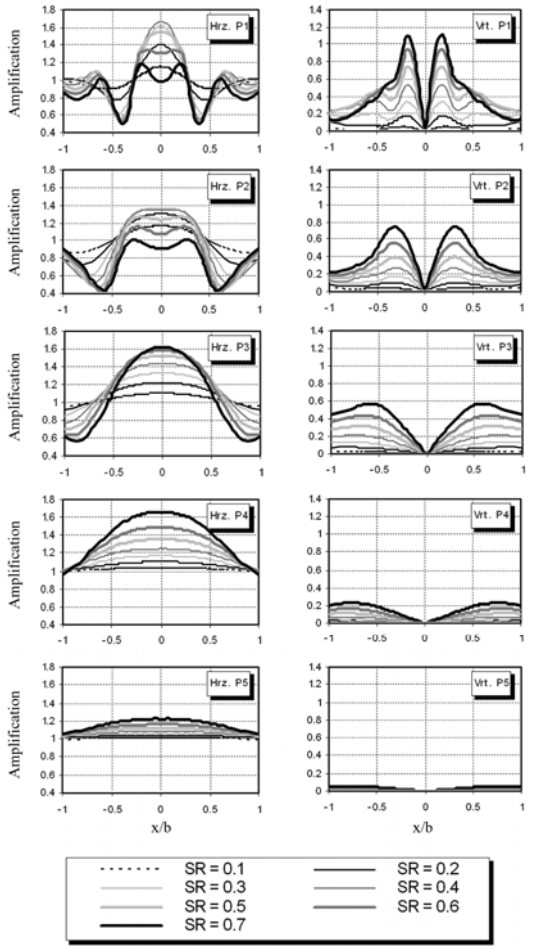

Figure 3. Grouping of amplification curves of the hill with shape ratio in the case incident SV wave and Poisson's ratio of 0.33

Wave Length Effect

Considering figure 3, irrespective of the shape ratio, the wave length plays a key rule in determining the amplification curve of the hill. Regarding the horizontal component, if the incident wave possesses a long or very long wave length, each point across the hill would experience amplification factor of greater than one, which increases with the shape ratio. In this case, the maximum amplification factor occurs at the top of the hill and the amplification curve decays toward the bases. In the case of an

incident wave with a medium wave length, although the same behavior would be seen, but some deamplification would also occur at the bases, whose magnitude increases with the shape ratio. In the case of an incident wave with a short or very short wave length, the number of deamplification zones along the hill would increase. In this case each point across the hill experiences its maximum amplification factor for a shape ratio of medium size and amplification curves corresponding to shape ratios of less than 0.6 experiences their maximums at points on the flank instead of the crest of the hill. Regarding the vertical component, irrespective of the shape ration, amplification curves start from a value of zero at the top, increase with distance from the crest; reach their maximum at a point on the flank and decay towards the base. In general and at any point across the hill, the vertical amplification factor increases with the shape ratio and decreases by increasing the wave length.

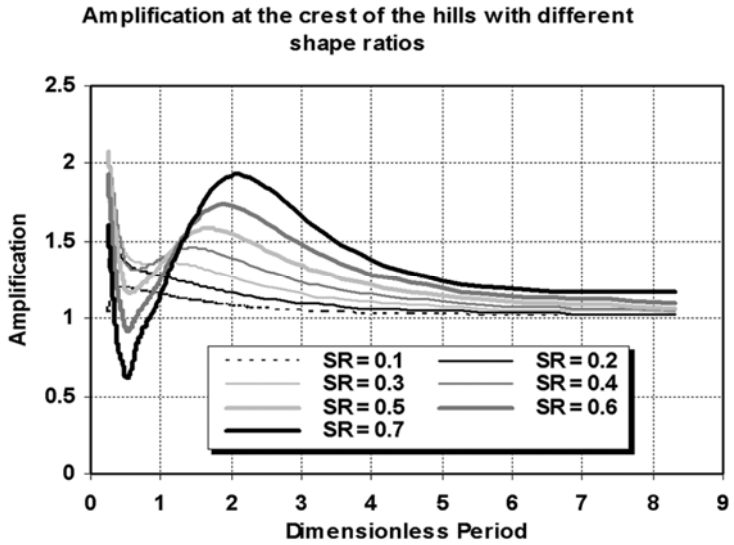

Figure 4. Amplification curves of the crest of the hill via different shape ratios in the case of incident SV wave and Poisson's ratio of 0.33

Wave Type Effect

Considering figure 2 shows that although the amplification patterns of 2D semi-sine shaped hills subjected to vertically propagating SV and P waves seem to be similar in general, but in the case of incident SV waves, larger amplification potentials are observed and larger frequency intervals are affected. Figure 5 categorizes the amplification patterns of 2D semi-sine shaped hills with a Poisson's ratio of 0.33, subjected to vertically incident P waves, according to their wave lengths. Both of horizontal and vertical components of amplification are shown. Comparison of figures 5 and 3 shows that in the case of incident P waves, unlike the case of incident SV waves, the amplification (or deamplification) factor of any point across the hill increases with the increasing shape ratio, irrespective of the incident wave's length. Also, in the case of incident P waves, unlike the case of incident SV waves, the maximum amplification factor occurs at the top of the hill, unless the incident wave possesses a very short wave length.

Poisson's Ratio Effect

For reason of simplicity, the mean amplification factor of the hill, defined as average of the amplification factors along the hill, was computed for investigation of the Poisson's ratio effect. Due to engineering points of view, amplification factors of less than one were substituted by one, in the averaging procedure. Figure 6 shows the variation of the mean amplification factor of the hill with the Poisson's ratio, versus different shape ratios and wave lengths, in both cases of incident P and SV waves. As can be seen, the Poisson's ratio has a secondary effect on the hill's amplification, compared to the shape ratio, wave length and wave type. In the case of hills with small shape ratios (< 0.2), the Poisson's ratio effect could actually be ignored, regardless of the incident wave length. In the case of hills with greater shape ratios, the Poisson's ratio effect could also be ignored, unless the incident

wave possesses a length of medium or smaller size. As expected, in the case incident waves with predominant periods of higher than the characteristic period, the amplification factor decreases as the Poisson's ratio increases.

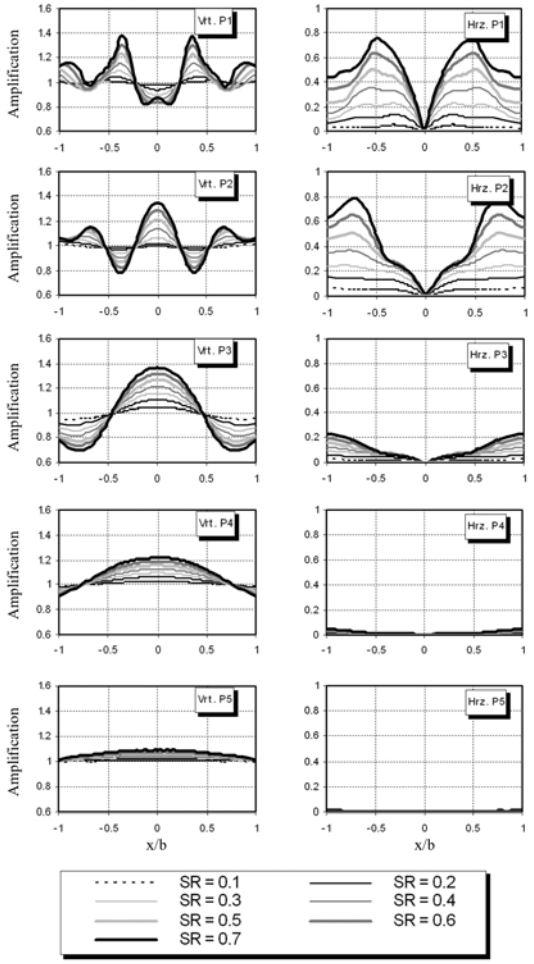

Figure 5. Grouping of amplification curves of the hill with shape ratio in the case incident P wave and Poisson's ratio of 0.33

ENGINEERING APPLICATIONS

Figure 7 presents a schematic view of some typical sites encountered in conventional seismic microzonation studies. Points A, B and C indicate, respectively, the ground surface of a soil stratum consisting of multiple layers with different properties overlying the bedrock, an arbitrary point along the homogenous rocky hill and the reference site on the rocky half space far away from the hill. In the current practice of 1D seismic microzonation, all homogenous rocky and rock like sites, irrespective of being located on top of the hills (point B) or on flat ground surface of the half space (point C), are regarded as similar reference sites without any amplification potential. The results presented in this paper indicate that this kind of treatment, even with homogenous hills, is neither accurate nor conservative. They encourage one to go a step forward in 1D site effect microzonation of topographical areas by distinguishing the amplification patterns of homogenous hills (point B) and free field half space (point C), conservatively.

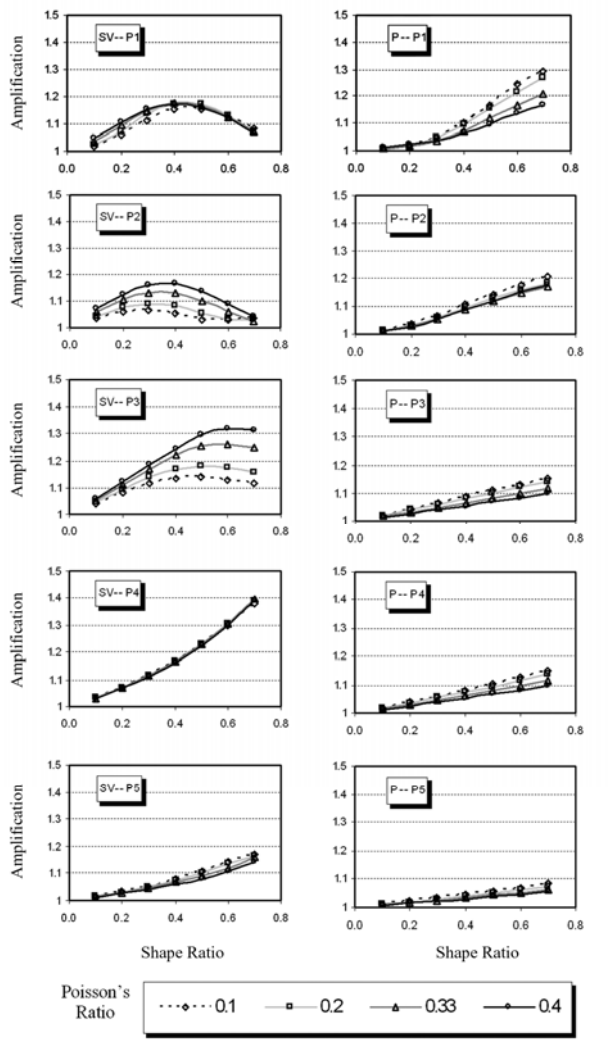

Figure 6. Mean amplification ratio of the hill via different Poisson's ratios

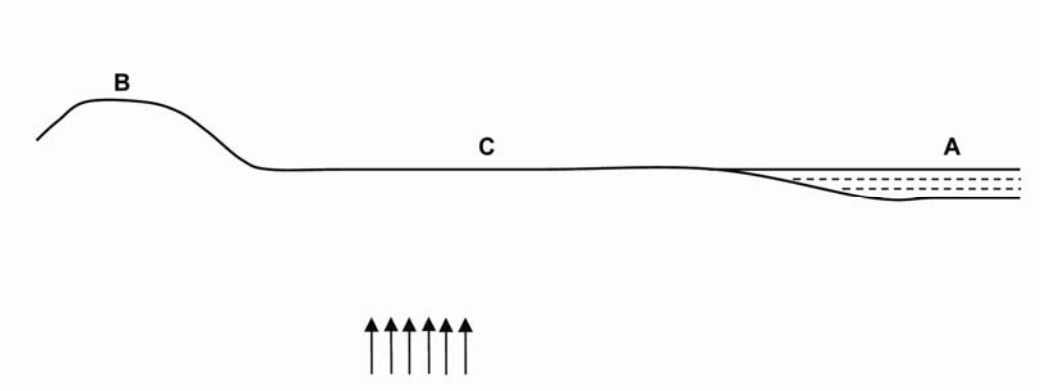

Figure 7. A schematic view of different site effect conditions subjected to the same incident waves

The dimensionless characteristic period of a 2D semi-sine shaped hill (T_C), which is the most important factor governing its seismic behavior, can be approximated as a function of only its shap-ratio (SR), that demonstrates the average characteristic period due to corresponding different Poisson's ratios:

$$T_C = 2.9(SR)^{0.7} \tag{4}$$

Tables (1) and (2) present, respectively, the mean horizontal and vertical amplification factors of a 2D homogenous semi-sine shaped hill as functions of its only shape-ratio and the predominant dimensionless period of the incident wave, which demonstrate the average amplification factors due to corresponding different Poisson's ratios. As can be seen, in the case of hills with shape ratios of more than 0.3, there are more than one period subinterval in which the average horizontal amplification factor exceeds 1.2. In other words, keeping in mind Borcherdt (1994) idea that the well known short and long period seismic coefficients (Fa and Fv) are strongly influenced by the amplification values averaged over the 0.1 to 0.5s and 0.4 to 2.0s periodic intervals, structures to be located along the hills should be designed to resist seismic forces of at least 20 percent larger than those corresponding to the flat free field half-plane.

Using the above mentioned relation and tables and having a knowledge of the base, height and shear wave velocity of semi-sine shaped existent hills throughout an area, the site period distribution map and also the period dependent amplification potential distribution maps obtained by 1D methods, could be easily modified.

Table 1. Horizontal amplification factors

SR	Dimensionless Periodic Range				
	P1	P2	P3	P4	P5
0.1	1.0	1.1	1.1	1.0	1.0
0.2	1.1	1.1	1.1	1.1	1.0
0.3	1.2	1.2	1.2	1.1	1.1
0.4	1.2	1.2	1.2	1.2	1.1
0.5	1.2	1.1	1.3	1.2	1.1
0.6	1.1	1.1	1.3	1.3	1.1
0.7	1.1	1.0	1.3	1.4	1.2

Table 2. Vertical amplification factors

SR	Dimensionless Periodic Range				
	P1	P2	P3	P4	P5
0.1	0.1	0.1	0.0	0.0	0.0
0.2	0.1	0.1	0.1	0.0	0.0
0.3	0.2	0.2	0.2	0.1	0.0
0.4	0.3	0.3	0.3	0.1	0.0
0.5	0.4	0.3	0.4	0.1	0.0
0.6	0.4	0.4	0.5	0.2	0.0
0.7	0.5	0.5	0.6	0.3	0.1

CONCLUSION

This paper presents clear perspectives of amplification patterns of 2D homogenous semi-sine shaped hills subjected to vertically propagating SV and P waves, by numerically investigation of the hill's response using the time domain boundary element method. It is shown that at:

- The amplification potential of the hill is strongly influenced by the length of the incident wave, by the shape ratio and in a less order of importance by the wave type and by the Poisson's ratio of the media.

- Every hill has a characteristic period that controls its seismic response. If the incident wave has a predominant period of equal to the characteristic one, all points along the hill show in-phase motions and its amplification potential reaches the maximum, which could be nearly equal to 2.0 in the case of a shape ratio equal to 0.7.
- In the case of incident waves with lengths of longer than the width of the hill, where the predominant periods are usually equal to or greater than its characteristic period, the amplification curve finds its maximum at the crest and decrease towards the base of the hill.
- In the case of incident waves with smaller lengths, some deamplification zones would occur along the hill whereas the maximum amplification potential could occur along the flank.

Simple formula and tables are proposed for evaluating the characteristic site period as well as the period dependent mean amplification potential of semi-sine shaped hills, which could be applied in seismic microzonation studies.

REFERENCES

Aki K and Larner K. "Surface motion of a layered medium having an irregular interface due to incident plane SH waves," Journal of Geophysical Research , 75, 933-954, 1970.

Ashford SA, Sitar N, Lysmer J and Deng N. "Topographic Effects on the Seismic Response of Steep Slopes," Bull Seismol Soc Am, 87, 701-709, 1997.

Association Française du Genie Parasismique (AFPS). Recommandations de la AFPS. Paris: AFPS. 183 pp., 1990.

Athanasopoulos GA, Pelekis PC and Leonidou EA. "Effects of Surface Topography on Seismic Ground Response in the Egion (Greece) 15-6-1995 Earthquake," Soil Dynamics and Earthquake Engineering, 18, 135-149, 1999.

Bard PY, "Effects of surface geology on ground motion: recent result and remaining issues," Proc. 10th European Conf. on Earthq. Eng., Vienna, 305-323, 1994.

Beskos DE. Boundary element methods in dynamic analysis: Pt. II (1986-1996), Appl Mech Rev, 50, 149-197, 1997.

Boore DM. "The effect of simple topography on seismic waves: implications for the accelerations recorded at Pacoima Dam, San Fernando Valley, California," Bull Seismol Soc Am, 63, 1603-1609, 1973.

Borcherdt RD. "Estimates of site-dependent response spectra for design (Methodology and Justification)," Earthquake Spectra, 10, 617-653, 1994.

Bouchon M. "Effect of Topography on Surface Motion," Bull Seismol Soc Am, 63, 615-632, 1973.

Bouchon M, Schultz CA, Toksos MN. "Effect of Three-Dimensional Topography On Seismic Motion," Journal of Geophysical Research, 101, 5835-5846, 1996.

Bouckovalas GD and Kouretzis G. "Review of Soil and Topography Effects in the September 7, 1999 Athens (Greece) Earthquake," Proceedings of the Fourth International Conference on Recent Advances in Geotechnical Earthquake Engineering and Soil Dynamics And Symposium in Honor of Professor WD Liam Finn, San Diego, California, 2001.

Bouckovalas GD and Papadimitriou AG. "Numerical evaluation of slope topography effects on seismic ground motion," Soil Dynamics and Earthquake Engineering, 25, 547-558, 2005.

Celebi M. "Topographical and geological amplifications determined from strong-motion and aftershock records of the 3 March 1985 Chile earthquake," Bull Seismol Soc Am, 77, 1147-1167, 1987.

Celebi M. "Topographic and geological amplification: Case studies and engineering implications," Structural Safety, 10, 199-217, 1991.

Dravinski M and Mossessian TK. "Scattering of plane harmonic P, SV, and Reyleigh waves by dipping layers of arbitrary shape," Bull Seismol Soc Am, 77, 212-235, 1987.

Eurocode8 (EC8), Design provisions for earthquake resistance of structures, 1998.

Geli L, Bard PV, Julien B. "The effect of topography on earthquake ground motion: a review and new results," Bull Seismol Soc Am, 78, 42-63, 1988.

Kamalian M. “Time Domain Two-Dimensional Hybrid FEM / BEM Dynamic Analysis of Non-Linear Saturated Porous Media,” Ph.D. Dissertation, Tehran University, 2001.

Kamalian M, Gatmiri B, Sohrabi-Bidar A. “On Time-Domain Two-Dimensional Site Response Analysis of Topographic Structures by BEM,” Journal of Seismology and Earthquake Engineering, 5, 35-45, 2003.

Kamalian M, Jafari MK, Sohrabi-Bidar A, Razmkhah A, Gatmiri B. “Time-Domain Two-Dimensional Site Response Analysis of Non-Homogeneous Topographic Structures by A Hybrid FE / BE Method,” Soil Dynamics and Earthquake Engineering, 26, 753-765, 2006.

Komatitsch D and Vilotte JP. “The spectral element method: an efficient tool to simulate the seismic response of 2D and 3D geological structures,” Bull Seismol Soc Am, 88, 368-392, 1998.

Kawase H. “Time-domain response of a semi-circular canyon for incident P, SV and Rayleigh waves calculated by the discrete wavenumber boundary element method,” Bull Seismol Soc Am, 78, 1415–1437, 1988.

Mossessian TK and Dravinski M. “Application of a hybrid method for scattering of P, SV, and Reyleigh waves by near-surface irregularities,” Bull Seismol Soc Am, 77, 1784-1803, 1987.

Sanchez-Sesma FJ and Campillo M. “Diffraction of P, SV and Rayleigh waves by topographic features: a boundary integral formulation,” Bull Seismol Soc Am, 81, 2234-2253, 1991.

Sanchez-Sesma FJ, Palencia VJ and Luzon F. “Estimation of local site effects during earthquakes: an overview,” ISET Journal of Earthquake Technology, 39, 167-193, 2002.

Spudich P, Hellweg M and Lee WHK. “Directional topographic site response at Tarzana observed in aftershocks of the 1994 Northridge, California, Earthquake: Implications for mainshock motions,” Bull Seismol Soc Am, 86, S139-S208, 1996.

Trifunac MD and Hudson DE. “Analysis of the Pacoima Dam accelerograms – San Fernando earthquake of 1971,” Bull Seismol Soc Am, 61, 1393-1411, 1971.

Wong HL. “Effects of surface topography on the diffraction of P, SV and Rayleigh waves,” Bull Seismol Soc Am, 72, 1167-1183, 1982.